

**Long-Range Ordered Phases without Short-Range Correlations**

V. K. Kabra and Dhananjai Pandey

*School of Materials Science and Technology, Banaras Hindu University, Varanasi 221 005, India*

(Received 15 April 1988)

We present results of Monte Carlo simulations of kinetics of spinodal ordering on a one-dimensional Ising chain with competing interactions up to third neighbors for Glauber and Kawasaki dynamics. Application of these results to the 2*H*-6*H* transformation in SiC shows that the arrested state of the transformation possesses long-range order but lacks short-range correlations.

PACS numbers: 61.50.Ks, 64.70.Kb, 81.30.Kf

Solid-state transformations from one close-packed modification to another in materials like SiC, ZnS, CdI<sub>2</sub>, cobalt and its alloys,<sup>1</sup> and martensites of copper-based alloys<sup>2,3</sup> take place through nucleation and propagation of stacking faults on the basal plane. These transformations often get arrested much before completion because of the formation of domains of the product phase in different orientations.<sup>4,5</sup> The arrested state has generally been described as a heavily disordered state because of the presence of extensive diffuse streaking along *c*\* for *HKL* reciprocal-lattice rows with  $H - K \neq 0 \pmod{3}$  (Ref. 6) on the diffraction patterns. The diffuse streaking does not disappear even after repeated annealings. Recently we have undertaken<sup>7</sup> a detailed Monte Carlo simulation study of the kinetics of domain formation and growth during the 2*H* to 6*H* transformation in SiC which is known<sup>4,5</sup> to take place above 1600°C. In this Letter, we show that the arrested state for the 2*H* to 6*H* transformation possesses long-range ordering but lacks any short-range correlation in the direction of stacking of the close-packed layers. As such, the arrested state for the 2*H* to 6*H* transformation cannot be categorized as a conventional crystal or glass.

The stacking sequence of a close-packed structure, in which atoms may lie in one of the three positions *A*, *B*, or *C*, can also be described<sup>8</sup> in terms of two state variables + and - which represent relative orientations of the pairs of consecutive layers and which for our purpose correspond to up (↑) and down (↓) Ising spins.<sup>9</sup> In this notation, pairs like *AB*, *BC*, *CA* and *BA*, *CB*, *AC* are represented by + and - symbols, respectively. The 2*H* (*AB*, ...) and 6*H* (*ABCACB*, ...) stacking sequences may therefore be described as containing ⟨1⟩ and ⟨3⟩ bands, where the numeral within the angular brackets is obtained by addition of all the consecutive spins of the same orientation.<sup>9</sup> Consider the Hamiltonian given below with competing interactions between the Zhdanov-Ising spins in the direction of stacking:

$$H = -\sum_r \sum_i S_i S_{i \pm r} J_r, \quad S_i = \pm 1. \tag{1}$$

The phase diagrams for this Hamiltonian with  $r=1, 2$ , and 3 are known.<sup>9,10</sup> Both the 2*H* ⟨1⟩ and 6*H* ⟨3⟩ phases appear simultaneously<sup>10</sup> for  $r=3$  only, and the corre-

sponding phase diagram is given in Fig. 1.

In order to study the temporal evolution of the 6*H* ⟨3⟩ bands as a 2*H* ⟨1⟩ crystal is quenched to the stability field of 6*H*, we have mapped the deformation and layer-displacement faults postulated by Pandey, Lele, and Krishna<sup>11</sup> for the 2*H* to 6*H* transformation into Glauber and Kawasaki dynamics, respectively. Transformation by the insertion of deformation faults (DF) will be martensitic in nature since it involves the shearing of parts of the crystal past each other across the slip plane (shown below by the vertical line). This is equivalent to a single spin flip as shown below: perfect 2*H* structure—

$$\dots A^+ B^- A^+ B^- | A^+ B^- A^+ B^- \dots,$$

2*H* with single DF—

$$\dots A^+ B^- A^+ B^+ | C^+ A^- C^+ A^- \dots$$

On the other hand, a layer-displacement fault (LDF) which causes a change in the orientation of a single close-packed layer (underlined layer shown below) is equivalent to the exchange of a pair of spins with total spin conserved<sup>12</sup>: perfect 2*H* structure—

$$\dots A^+ B^- A^+ B^- \underline{A^+ B^-} A^+ B^- \dots,$$

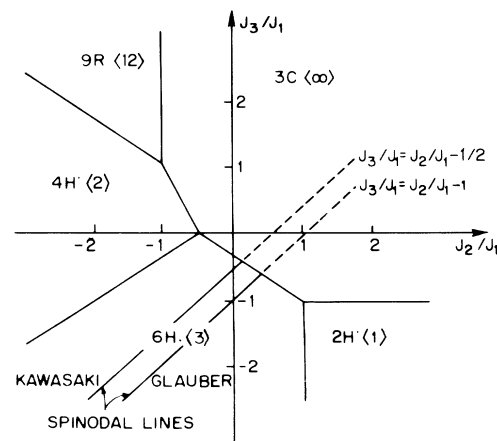


FIG. 1. Phase diagram of an Ising chain with interactions up to third neighbor ( $J_1 > 0$ ). After Ref. 10.

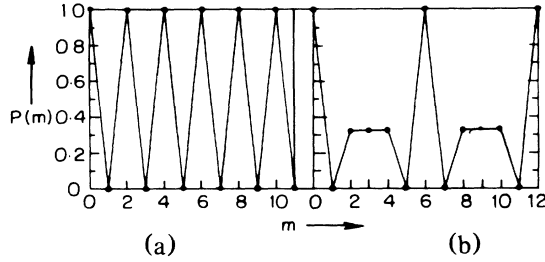


FIG. 2. Pair correlations for the perfect (a) 2H and (b) 6H structures.  $P(m)$  is defined at integer values of  $m$ . The continuous lines are drawn as guides to the eyes.

2H with single LDF—

$$\dots A^+B^-A^+B^+C^-B^-A^+B^- \dots$$

The temporal evolution of 6H domains as a 2H crystal is quenched to the stability field of 6H will depend on whether 2H is metastable or unstable.<sup>13</sup> The condition for spontaneous spin flip or exchange (spinodal ordering) to take place at 0 K without any nucleation barrier for the Hamiltonian given by Eq. (1) with  $r=3$  is

$$\frac{\Delta H}{J_1} = \frac{J_3}{J_1} - \frac{J_2}{J_1} - 1 \leq 0 \quad (\text{Glauber dynamics}),$$

$$\frac{\Delta H}{J_1} = \frac{J_3}{J_1} - \frac{J_2}{J_1} - \frac{1}{2} \leq 0 \quad (\text{Kawasaki dynamics}).$$

These conditions fix the spinodal line which separates the metastable and unstable 2H regimes for the two dynamics under consideration. We have studied the dynamical evolution of the 6H domains at 0 K in the spinodal regime with  $J_3/J_1 = J_2/J_1 = -\frac{1}{2}$  via the standard Monte Carlo technique. For this, we select the sites in an ensemble of 1200 layers using pseudorandom numbers [1,1200] and then effect the spin flip or exchange if the energy cost of the process at the selected site is zero or negative. We have monitored the average 6H domain size, number of 6H clusters, excess energy over the 6H ground state, and three pair correlation functions as functions of time, where the unit of time is taken as one Monte Carlo attempt-step per site (MCS/s). If we define  $P(m)$ ,  $Q(m)$ , and  $R(m)$  as the probabilities of finding  $AA$ ,  $BB$ ,  $CC$ ;  $AB$ ,  $BC$ ,  $CA$ ; and  $AC$ ,  $BA$ ,  $CB$  type pairs of layers with  $m$ -layer separation, respectively, the diffracted intensity from a stack of  $N$  layers can be expressed as<sup>6,14</sup>

$$I(h_3) = N + 2 \sum_{m=1}^{N-1} (N-m) [J'_m \cos m\phi - J''_m \sin m\phi], \quad (2)$$

where

$$J'_m + iJ''_m = P(m) + Q(m) \exp(-i\theta) + R(m) \exp(i\theta),$$

$\theta = 2\pi(H-K)/3$ , and  $\phi = \pi h_3$ , with  $h_3$  being the continuous variable along  $c^*$ . The pair correlations  $P(m)$ ,

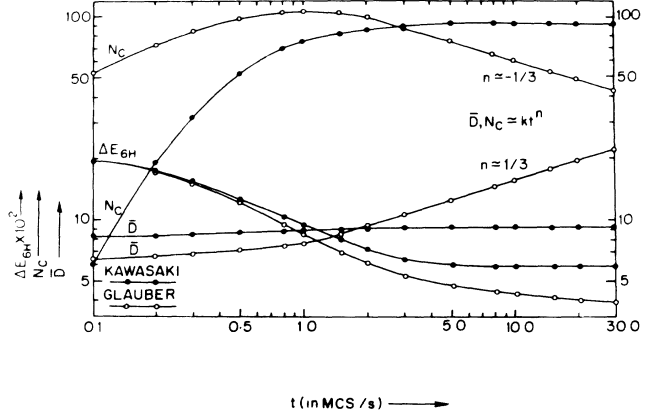


FIG. 3. Variation of mean 6H domain size ( $\bar{D}$ ), number of 6H clusters ( $N_c$ ), and excess energy over the 6H ground state ( $\Delta E$ ) with time in MCS/s. Curves marked with  $\bullet$  and  $\circ$  correspond to Kawasaki and Glauber dynamics, respectively. Note that  $\bar{D}$ ,  $N_c$ , and  $\Delta E$  level off beyond 8 MCS/s for the Kawasaki dynamics. For the Glauber dynamics, the temporal evolution of  $\bar{D}$  follows a power law with a growth exponent of  $\frac{1}{3}$  at late times.

$Q(m)$ , and  $R(m)$  have fixed periodic values for  $m = 0, 1 \pmod{2}$  and  $m = 0, 1, 2, 3, 4, 5 \pmod{6}$  for the perfect 2H and 6H structures, respectively [see Figs. 2(a) and 2(b)]. This is not so for the faulted crystal and we have monitored the time evolution of these pair correlations in our simulation studies.

Figure 3 depicts the time evolution of the mean domain size, the number of 6H clusters, and the excess energy over the 6H ground state, as determined by averaging over 50 configurations for the two dynamics. It is evident from Fig. 3 that for the Kawasaki dynamics, the configuration freezes just beyond 8 MCS/s with a mean domain size of  $\sim 9$  layers. Since the concept of unit cell for the average structure would have been valid if the 6H unit cell could repeat itself at least once, i.e., if the mean domain size were over 12 layers, an average domain size of  $\sim 9$  layers implies a lack of short-range ordering. This is confirmed by the behavior of pair correlation  $P(m)$  obtained by averaging over 1000 configurations, shown in Fig. 4(a). A comparison of the short-range correlations in Fig. 4(a) with those given in Figs. 2(a) and 2(b) for the perfect 2H and 6H structures clearly shows that the frozen configuration lacks short-range ordering. Intriguingly, the frozen configuration cannot be termed glassy<sup>15</sup> either, since it still possesses long-range ordering beyond  $m = m' = 12$ . This is thus in sharp contrast to the glassy frozen systems observed<sup>15</sup> in binary alloys undergoing phase separation after being quenched to zero temperature. Let  $P_e$  and  $P_o$  be the values to which  $P(m)$  converges for  $m$  even and odd, respectively, beyond  $m = m'$  that manifests the long-range ordering. After simple mathematical manipulations, Eq.

(2) now reduces to (for  $N \gg p$ )

$$\begin{aligned}
 I(h_3) = & 1 - N + \sum_{p=1}^{(m'-1)/2} (N - 2p) [3\{P_e(2p) - P_e\} \cos 2p\phi + 2J''_{2p} \sin 2p\phi] \\
 & + \sum_{p=1}^{(m'-1)/2} (N - 2p - 1) [3\{P_o(2p+1) - P_o\} \cos(2p+1)\phi + 2J''_{2p+1} \sin(2p+1)\phi] \\
 & + N^{-1} \{ (3P_e - 1) \sin^2[\frac{1}{2}(N-2)\phi] / \sin^2\phi + (3P_o - 1) \cos\phi \sin^2[\frac{1}{2}(N-3)\phi] / \sin^2\phi \}.
 \end{aligned}
 \tag{3}$$

We have taken  $m'$  as odd and  $N$  as even numbers, and  $p$  varying as  $1 \leq p \leq (N-2)/2$ . Thus the presence of long-range ordering manifests itself through the sharp  $\delta$  peaks in reciprocal space at  $2H$  positions, with weights different from the perfect  $2H$  structure, as shown in Fig. 5(a) for various instants of time. The first two terms in Eq. (3) are responsible for the diffuse streak along  $c^*$  joining the  $\delta$  peaks as well as the elongated spots midway between the  $\delta$  peaks.

For the Glauber dynamics, there is clear late-stage domain growth and a concomitant decrease in the number of  $6H$  clusters due to Ostwald ripening after the initial spinodal ordering (see Fig. 3). We have verified the late-stage domain growth up to 1000 MCS/s. Also, the three pair correlations converge to  $\frac{1}{3}$  for values which gradually increase with time as can be seen from Fig. 4(b) for  $P(m)$ . The convergence of pair correlations to

$\frac{1}{3}$  implies<sup>6</sup> that the probability of finding the  $m$ th layer in  $A, B,$  or  $C$  orientation has become equal, indicating total absence of long-range ordering. The Fourier transforms of the pair correlations computed at various intermediate stages of transformation using Eq. (2) are shown in Fig. 5(b). It is evident from this figure that, unlike for Kawasaki dynamics, the transformation commences with an initial broadening of  $2H$  reflections. At

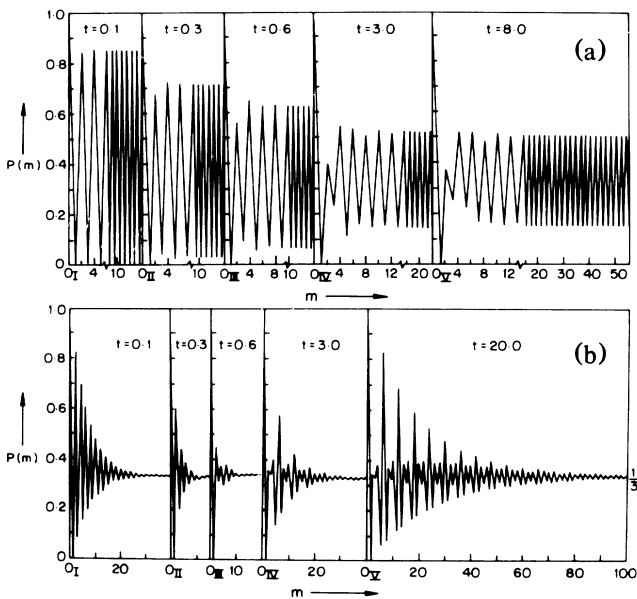


FIG. 4. Variation of pair correlations with time for (a) Kawasaki dynamics and (b) Glauber dynamics. For the Kawasaki dynamics, the scale for  $m$  is condensed beyond the point marked by a break. Note the regularity in  $P(m)$  beyond this break point.  $O_I$  to  $O_V$  are the origins at the five instants of time in both the figures. Short-range correlations corresponding to a six-layer repeat period can be easily seen in Fig. 4(b) at  $t=20.0$  MCS/s. The short-range correlations at  $t=8.0$  MCS/s corresponding to the frozen configuration shown in Fig. 4(a) do not show any translational periodicity.

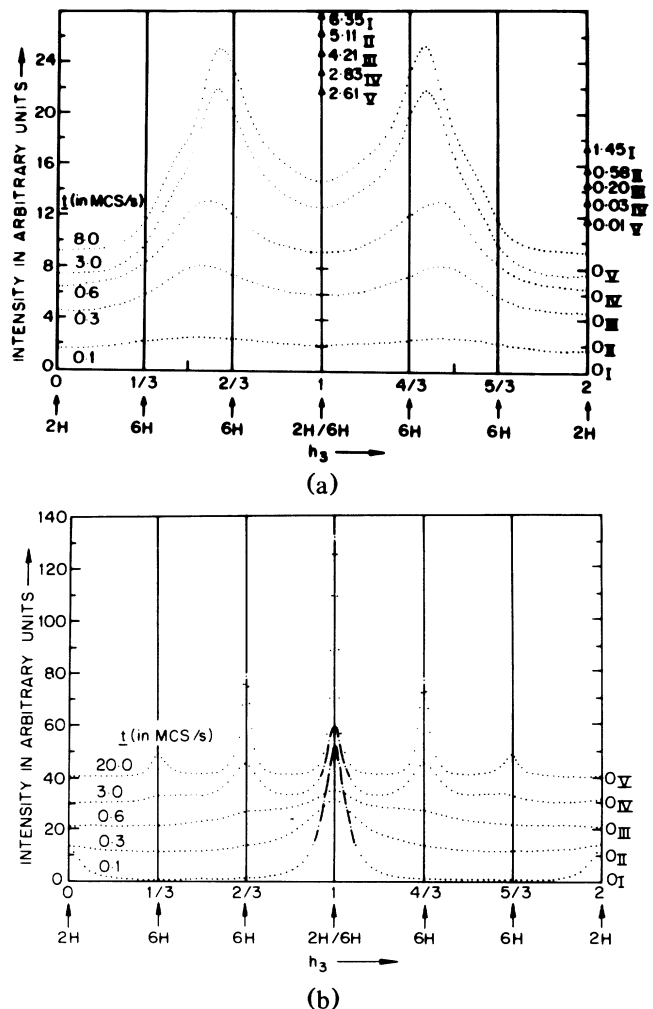


FIG. 5. Intensity distributions along diffuse streak for (a) Kawasaki dynamics and (b) Glauber dynamics at various instants of time.

a later stage, diffuse  $6H$  reflections near  $h_3 = \pm \frac{1}{3}, \pm \frac{2}{3} \pmod{2}$  positions start appearing.

As shown elsewhere,<sup>16</sup>  $2H$  reflections are experimentally found to remain unbroadened during the  $2H$  to  $6H$  transformation in SiC although their intensities do change. Further, diffuse elongated spots approximately midway between the  $2H$  reflections develop in the course of transformation. Both of these observations are in perfect agreement with the theoretically computed intensity distribution shown in Fig. 5(a) for the Kawasaki dynamics. The experimentally observed diffuse elongated spots do not split into the distinct  $6H$  reflections even after repeated annealings, confirming the arrest of transformation which can be explained in terms of Kawasaki dynamics only, since for the Glauber dynamics there is a clear late-stage domain growth. In the light of the temporal evolution of pair correlations given in Fig. 4(a) for the Kawasaki dynamics, we may thus conclude that the arrested state for the  $2H$  to  $6H$  transformation in SiC possesses long-range ordering but lacks any short-range correlation in the direction of stacking of close-packed layers. The lack of short-range ordering in the frozen configuration is actually due to the frustration introduced by the extended metastability of the  $4H$  phase deep in the  $6H$  phase field up to  $J_2/J_1 = \frac{1}{2}$  with respect to spin-exchange dynamics: Spin exchange at an isolated site leads to local  $4H$  ordering (two 2 bands) which once formed can exist metastably unless and until spin exchange takes place at three-site separation from the earlier site transforming the  $4H$ -like ordering region into  $6H$ . On the other hand, the spin-flip dynamics can only lead to a 3 band in one step, and hence there is no frustration.

One of us (D.P.) is extremely thankful to Professor T. V. Ramakrishnan for providing the encouragement and guidance at various stages of this work. The stimulating discussions with him and Dr. S. Lele, Dr. J. Yeomans, Dr. S. Jain, Dr. H. R. Krishnamurthy, Dr. C. Dasgupta, Dr. D. Kumar, Dr. S. Shenoy, Dr. M. Barma, and Dr. D. Dhar are gratefully acknowledged. One of us (D.P.) is grateful to Homi Bhabha Fellowships Council and the

other (V.K.K.) is grateful to the University Grants Commission for the award of fellowships. We are extremely thankful to Professor S. Ranganathan for providing the computational facilities.

<sup>1</sup>D. Pandey and P. Krishna, in *Current Topics in Materials Science*, edited by E. Kaldis (North-Holland, Amsterdam, 1982), Vol. 9.

<sup>2</sup>L. Delaey *et al.*, in *Proceedings of an International Conference on Solid to Solid Phase Transformations, Pittsburgh, Pennsylvania, 1981*, edited by H. I. Aaronson *et al.* (AIME, New York, 1982).

<sup>3</sup>V. K. Kabra, D. Pandey, and S. Lele, *Acta Metall.* **36**, 725 (1988).

<sup>4</sup>P. Krishna and M. C. Marshall, *J. Cryst. Growth* **9**, 319 (1971).

<sup>5</sup>P. Krishna and M. C. Marshall, *J. Cryst. Growth* **11**, 147 (1971).

<sup>6</sup> $HK.L$  reflections with  $H - K = 0 \pmod{3}$  are not affected by faulting. For details, see A. J. C. Wilson, *X-Ray Optics* (Methuen and Co., London, 1962), Chap. 5.

<sup>7</sup>V. K. Kabra and D. Pandey, to be published.

<sup>8</sup>G. S. Zhdanov and Z. V. Minervina, *J. Phys. USSR* **9**, 151 (1945).

<sup>9</sup>J. Yeomans, in *Solid State Physics*, edited by H. Ehrenreich, F. Seitz, and D. Turnbull (Academic, Orlando, 1987), Vol. 41.

<sup>10</sup>W. Selke, M. Barreto, and J. Yeomans, *J. Phys. C* **18**, L393 (1985).

<sup>11</sup>D. Pandey, S. Lele, and P. Krishna, *Proc. Roy. Soc. London A* **369**, 435, 451 (1980).

<sup>12</sup>We are thankful to Dr. H. R. Krishnamurthy for pointing out this equivalence.

<sup>13</sup>J. D. Gunton, M. San Miguel, and P. S. Sahni, in *Phase Transitions and Critical Phenomena*, edited by C. Domb and J. L. Lebowitz (Academic, New York, 1983), Vol. 8.

<sup>14</sup>H. Holloway and M. S. Klamkin, *J. Appl. Phys.* **40**, 1681 (1969).

<sup>15</sup>S. A. Safran, P. S. Sahni, and G. S. Grest, *Phys. Rev. B* **28**, 2693 (1983).

<sup>16</sup>D. Pandey, S. Lele, and P. Krishna, *Proc. Roy. Soc. London A* **369**, 463 (1980).